Machine learning on multisensor data from airborne remote sensing to monitor plastic litter in oceans and rivers (PlasticObs+)

Christoph Tholen
German Research Center for Artificial Intelligence RG Marine Perception
Oldenburg, Germany
Christoph.Tholen@dfki.de

Mattis Wolf
German Research Center for Artificial Intelligence RG Marine Perception
Oldenburg, Germany
Mattis.Wolf@dfki.de

Carolin Leluschko
German Research Center for Artificial Intelligence RG Marine Perception
Oldenburg, Germany
Carolin.Leluschko@dfki.de

Oliver Zielinski
Leibniz Institute for Baltic Sea Research Warnemünde and German Research Center for Artificial Intelligence RG Marine Perception
Oldenburg, Germany
Oliver.Zielinski@io-warnemuende.de

***Abstract*— This paper presents the main ideas and initial findings of the PlasticObs+ project. The long-term goal of the project is to develop an airborne based method for monitoring plastic waste on the water surface. For this project, aircrafts usually applied for oil spill detection are used. Plastic waste detection and analysis is achieved using artificial intelligence (AI) within four different AI-systems. Furthermore, results from field tests were used to determine the limits of detectability of plastic waste from different altitudes. It was shown that both color and size of the items have an influence on the detectability. In addition, the underground plays an important role. A binary classifier, based on a Convolutional Neural Network (CNN) was trained to distinguish between images containing plastic and those not polluted. The accuracy of the CNN was 93.3 % while the accuracy of the labels generated by humans was 92.6 %.**

Keywords*— *Artificial Intelligence, Plastic Waste Monitoring, Detection, Convolutional Neural Networks, Transfer Learning

I. INTRODUCTION

Plastic pollution is a 'hazardous environmental problem' with annual estimates indicating global rivers discharging several million metric tons of plastic waste into the oceans [1], [2]. To improve waste and plastic management, it is crucial to implement cost-effective and innovative monitoring strategies. These strategies should be based on scientifically proven research that identifies the sources and amounts of litter in different towns, states, and countries. Additionally, it is important to obtain information about the types of plastic litter, such as polymer types, to develop targeted policies, legislation, and investments for the collection and recycling of priority plastic items. These actions are consistent with major political initiatives, such as the EU Marine Strategy Framework Directive's descriptor 10 [3], the Single-use Plastics Directive 2019 [4], UN Sustainable Development Goal 14 target 14.1, and the UN Decade of Ocean Science for Sustainable Development (2021-2030), which all aim to reduce marine pollution and improve ocean health [5].

Funded by the German Federal Ministry for the Environment, Nature Conservation, Nuclear Safety and Consumer Protection (BMUV) based on a resolution of the German Bundestag (Grant No. 67KI21014A).

979-8-3503-3226-1 © 2023 IEEE

The detection of pollution on the ocean surface, such as oil spills or plastic debris, is of critical interest for the protection of marine ecosystems and the safety of human activities [6]. Although there have been some studies on the detection of plastic using remote sensing techniques in the past [7], [8], continuous monitoring of larger, contiguous marine areas as a first step of inventory and control has not been established yet. Knowledge to date is therefore essentially based on temporally and spatially punctual measurements. The highly inhomogeneous distribution of plastic allows only inadequate generalizations about the sources, distribution routes, and accumulation sites as well as their development over time. This circumstance is also frequently described in the literature [9], [10].

This is where the PlasticObs+ project comes in. The long-term goal of the project is to develop an airborne method for monitoring plastic waste on the water surface. For this project, aircrafts commonly used for oil spill detection are used. Those aircrafts are already in operation in different countries all over the world. The main idea of the PlasticObs+ project is to use the infrastructure already in operation and apply plastic waste assessment as an additional service. This will reduce operational costs for plastic waste assessment and prevent additional emissions caused by plastic waste monitoring.

System Overview

The PlasticObs+ system is based on an overview sensor, a fast edge AI for anomaly detection, an AI based system for candidate selection, and a detail sensor to further investigate the candidates selected (Fig. 1). A line scanner provides overview images of large areas with a low resolution of approx. 0.15 m/px for an altitude of 1000 ft. These overview images are then analyzed during the flight using an edge AI system to identify anomalies that may indicating plastic waste accumulations. The output of this first AI-system is used to select candidates which should be further investigated using the high-resolution imagery system (EOIR). The anomaly detection must be undertaken using a fast approach because the hotspots identified will be further investigated using the detail sensor within the same flight. Therefore, the decision which areas should be captured

by the EOIR needs to be taken within a few seconds. The resolution of the EOIR is approx. 0.03 m/px for an altitude of 1000 ft.

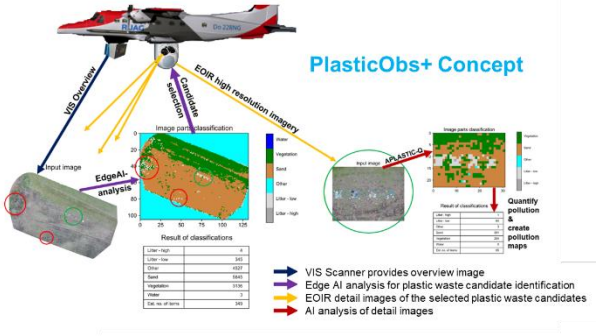

Fig. 1. Overview of Plastic Obs + concept

II. Artificial Intelligence Systems

The PlasticObs+ concept is relying on four different AI systems, further described within this section focusing on potential methods for the design of the systems.

A. VIS-AI

In a first step, the overview sensor takes a low-resolution image of the scene, which is evaluated with aid of the first AI system. The goal of this preliminary evaluation is to detect potential accumulations of litter, resulting in a heat map that is sent to the following candidate selection system. This heat map contains a value for each pixel of the input image that reflects the probability that the pixel contains litter. This pixel-wise classification can be solved using semantic segmentation methods.

In this particular application, a major challenge is an ability to evaluate the input images in real time, during the flight. While the use of deep neural networks for segmentation tasks shows great performance in terms of accuracy, they usually consist of a great number of learned weights, which makes them computationally heavy and slow in inference. Several methods have been proposed to make deep neural networks more efficient by compressing the network size and accelerating inference time. Examples of those methods are network pruning [11] or developing a network with a bilateral structure [12]. Another approach for finding a suitable network architecture, given the two conflicting goals of performance and low latency time, is the use of neural architecture search (NAS), as used for the development of FasterSeg [13].

Another challenge posed by the real-time VIS-AI system is the processing of low-resolution aerial imagery. The authors in [14] are targeting this problem by proposing a framework that extends the semantic segmentation with a super-resolution module to achieve better segmentation performance. As previously stated, the VIS-AI system must be capable of real-time inference, therefore it is necessary to investigate how the combination of super-resolution module and semantic segmentation affects the inference time.

B. Candidate Selection System

The output of the VIS-AI is a heatmap containing the positions of potential plastic waste hotspots, which should be further investigated using the EOIR sensor. However, due to limited time and movement capabilities of the EOIR the number of hotspots, which can be investigated by the EOIR per second, is limited. Therefore, an algorithm for selecting the most promising regions for investigation is needed. However, the criterion for selecting the region needs to be specified. For instance, there could be one region with a very high score, but far away from all other potential waste hotspots and, at the same time, a certain number of hotspots with a lower score but close together, so that all hotspots could be investigated.

The optimisation problem described can be understood as a cost-constrained traveling salesman problem (CCTSP) [15]. The CCTSP is an adaptation of the well-known traveling salesman problem (TSP) [16]. In CCTSP each city or node n is given a certain value v and a fixed cost-constrained B is defined [15]. The aim is to find a subtour including m nodes with $m \leq n$ that maximizes the total value, while the total costs does not exceed the given cost constraint B.

$$\sum_{i=1}^{m-1} C_{\pi(i),\pi(i+1)} + C_{\pi(m),\pi(1)} \leq B. \quad (1)$$

Where $C_{\pi(i),\pi(i+1)}$ denotes the cost to travel from node $\pi(i)$ to node $\pi(i+1)$ and $C_{\pi(m),\pi(1)}$ denote the cost to return from the last node back to the start node. A side condition in CCTSP is to maximize the sum of the values of the chosen subset:

$$max\left(\sum_{i=1}^{m} v_{\pi(i)}\right). \quad (2)$$

Where $v_{\pi(i)}$ represents the value of the node $\pi(i)$.

Dynamic programming or branch and bound methods can be used to generate an exact solution for the given CCTSP problem [17]. However, these approaches are time-consuming, and it cannot be guaranteed that a solution is available within the given time constraint. Instead, a heuristic approach is used in this research. Here a greedy algorithm, based on a nearest neighbor approach will be used to generate an initial solution. However, in cost constrained applications not only the distance between the nodes should be used to choose the next neighbor, rather the values of the different nodes should be considered. This can be achieved in different ways, for instance by using the linear combination of the distance between the nodes and the value of the new node [18] as follows:

$$d_i = C_{\pi(n),\pi(i)} \cdot v_{\pi(i)}. \quad (3)$$

Where $C_{\pi(n),\pi(i)}$ denotes the cost from the last node in the subset to the current node and $v_{\pi(i)}$ denotes the value of the current node. Another option is to take the ratio of the value of the next node and the distance between the last node and the next node [19] as follows:

$$d_i = \frac{v_{\pi(i)}}{c_{\pi(n),\pi(i)}}. \quad (4)$$

In both cases the weighted distance d_i is calculated for all open nodes, i.e., nodes which are not included in the subset so far, and the best option is chosen as next node and inserted into the subset.

Afterwards, an optimization algorithm, for example k-opt [20], [21], simulated annealing [22] or hill climbing [23] can be used to refine the initial solution generated by the greedy algorithm.

C. EOIR-AI

For the hotspots identified by the VIS-AI and chosen for investigation by the CSS high resolution images are captured using the EOIR. The images are stored and analyzed after the flight using the EOIR-AI system. Results of the analysis are then distributed via a Geographic Information System (GIS) (Fig. 2).

In recent research different well-established AI-methods were used for the identification and qualification of plastic litter in the marine environment. For instance, Random Forest classifiers (RF) were used by Martin et al. [24] and Gonçalves et al. [25] to recognize dry plastic items in the Red Sea and Portugal. Acuña-Ruz et al. [26] used Support Vector Machines (SVM) to detect ashore plastic in Chiloé islands. In addition, CNNs were used for plastic waste assessment. Bak et al. [27] used Visual Geometry Group 16 architecture while Kylili et al. [28] used SegNet architecture to detect beached and floating plastic litter. Wolf et al. [29] used a two-step CNN-based approach for the identification and qualification of marine plastic litter.

Within the PlasticObs+ project the approach described in [29] will be used as a starting point for the development of the EOIR-AI. The image taken by the EOIR only covers a small section of the area under investigation. Therefore, the data from the line scanner will be incorporated into the AI analysis, to support context extraction, for instance morphology extraction (Fig. 2).

In addition, explainable AI-methods (XAI) [30] will be incorporated in the EOIR-AI to provide the user with valuable information about the decision process.

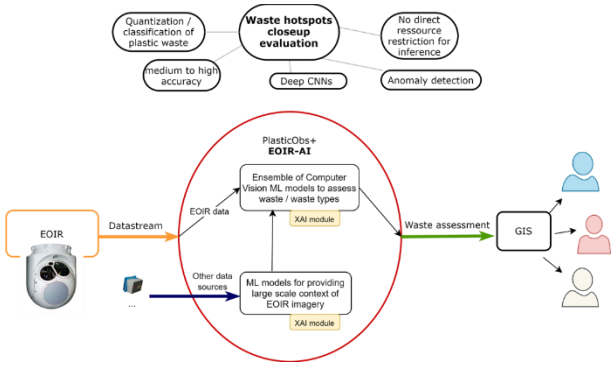

Fig. 2. System design of the EOIR AI

D. Feedback Loop

The selected candidate proposition output for the potential waste hotspots given by the VIS-AI (Section II.A) directs the EOIR to provide high-resolution imagery for the given potential waste hotspot. Together with the EOIR-AI (Section II.C) waste assessment outputs, this creates two data pairs of imagery and their corresponding predictions for the same spatial location, where the resolution of the EOIR imagery is around five times higher.

Initially, the imagery of the two data pairs will be used for enhanced annotation by human experts of the VIS-Line data for the VIS-AI. Because the imagery of the EOIR offers higher resolution, it will reduce the risk of making mistakes during the annotation process, because it can also be used for the decision-making process.

With increased capacities of both involved AI-systems (VIS-AI and EOIR-AI), a scaling up of annotation will be enabled trough semi-automatic labelling with a human expert in the loop, as depicted in Fig. 3 and described by Budd et al. [31]. This is expected to facilitate annotation, as the waste assessments of the EOIR-AI should allow to provide a selection of imagery suitable for annotation, in particular imagery of waste hotspots, to the expert in the loop. With a better performing EOIR-AI, it is expected to provide better suggestions for annotations for VIS line scanner data. This annotated VIS-data should then facilitate the performance to the VIS-AI after iterative optimizing throughout the project, and hence provide ultimately better suggestions for waste hotspots. This relates to Li et al. [32], and instead of super resolution imagery, the PlasticObs+ feedback loop uses real world data.

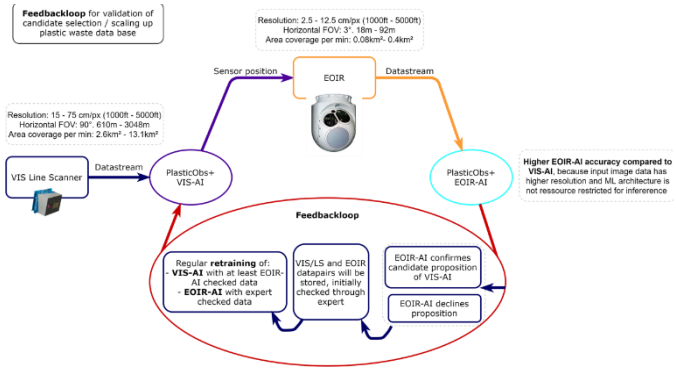

Fig. 3. System design of the feedback loop

III. Field Tests

In previous research, images from a lower altitude were used for plastic waste assessment, allowing to distinguish between different litter categories and the identification of small litter items like cup lids or food wrappers [29]. However, due to the higher altitude, images with a lower resolution will be used in this project. Therefore, a set of field tests was undertaken using artificial plastic waste targets to determine the limits of detectability for the problem at hand. The use of artificial targets to determine the limits of detectability of remote sensing applications was also applied by Topouzelis et al. [7].

The field tests were conducted between the 08th and the 10th of November 2022 on the island of Spiekeroog (southern North Sea). During the field tests different kinds of plastic, i.e. LDPE blue (low density Polyethylene), LDPE transparent, PS white (Polystyrene), PS cream and PP black (Polypropylene), were used to form artificial targets covering different percentages of one square meter, i.e. 100 % 50 %, 25 % 12.5 % and 6.25 %. In addition, the experiments were conducted at two different locations, covering two different kinds of soil, i.e grass and sand. The experimental setup at both locations is shown in Fig. 4.

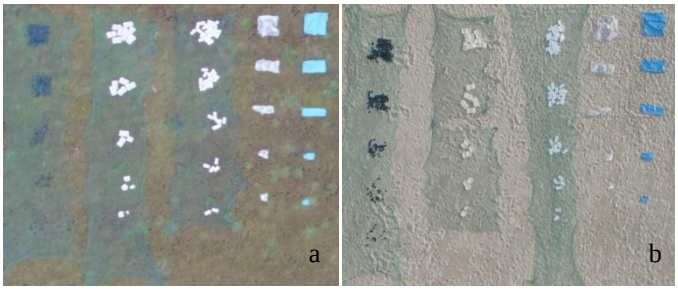

Fig. 4. Experimental set-up of the field tests on grass (a) and sand (b) soil

A research aircraft was used to take images of the experimental setup in different altitudes from the range 150 m to 1200 m. However, due to bad weather conditions, the maximum altitude for sand soil was 750 m. During postprocessing snippets only containing a single target were stored in a database. In addition, snippets not containing plastic were also inserted into the database. In total 450 snippets were produced, 360 containing plastic waste and 90 snippets not containing plastic waste. Fig. 5 shows examples from the snippet database for six different altitudes.

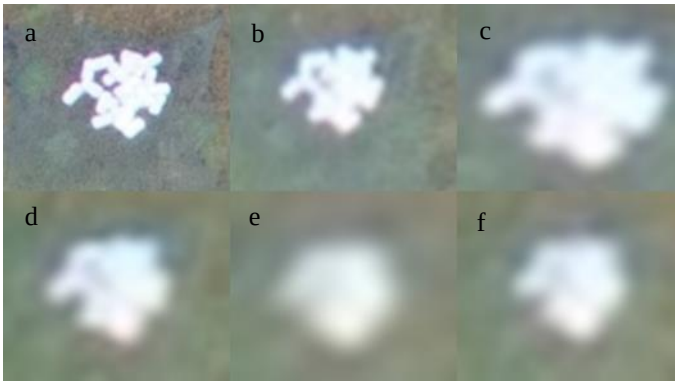

Fig. 5. Examples from snippet database showing PS white with 100 % coverage from altitude 150 m (a), 300 m (b), 450 m (c), 600 m (d), 800 m (e), 1000 m (f)

In order to determine the limits of detectability, all snippets were labelled by humans. During the labelling process the humans had to answer the questions if plastic is visible on the snippets or not. Each snippet was independently labelled by five humans. The results of the labelling process are presented in the next section.

In addition, a machine learning approach for classification was implemented. A convolutional neural network (CNN) was trained by adapting knowledge from an existing network and applying it to solve the given problem of classifying images containing plastic and not containing plastic. This approach is called transfer learning [33].

The machine learning approach is based on ResNet-50, a CNN containing 50 layers designed for image processing applications [34]. Based on the pre-trained layers and weights of this network, the CNN was finely tuned by changing the output layers to two classes: P*lastic* and *No Plastic*. Afterwards, the weights of the other layers were fixed, and the weights and biases of the newly added layers were trained.

The dataset was split into a training set and a test set. The training set contained 80 % of the images, while 20 % were used for testing. Training was limited to 10 epochs. Fig. 6 shows the accuracy and the loss over iterations for the training of the CNN.

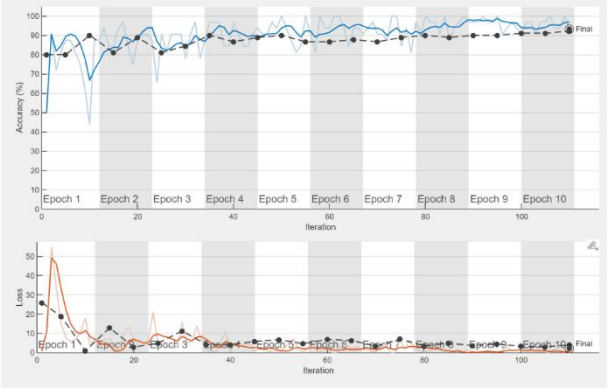

Fig. 6. Training results of ResNet 50 transfer learning

IV. Results

In this section the results from the field tests are presented focusing on the labelling process. For analysis the given answers are compared with the true labels of the snippets. In this research the accuracy is used as metric to evaluate the detectability. The accuracy is calculated as follows:

$$acc = \frac{TP}{N}. \tag{5}$$

Where *TP* denotes the correct labelled images, while *N* represents the number of images. Fig. 7 shows the accuracy as function of the altitude. Each plastic sort is evaluated separately. In addition, the accuracy of the snippets without plastic is shown. It can be seen from the figure that, on grass soil, the accuracy of all plastic sorts, except PP black, is higher than 0.88 regardless of the altitude. Furthermore, the accuracy of PP black shows a negative correlation with altitude. On sand soil LDPE transparent and PP black showed a constantly decreasing accuracy over altitude, while the accuracy of PS cream and PS white rapidly decreased for an altitude of 750 m. The accuracy of LDPE blue was not affected by higher altitudes. In addition, in both cases almost all snippets without plastic are labelled correctly. Unfortunately, no data is available for higher altitudes due to bad weather conditions.

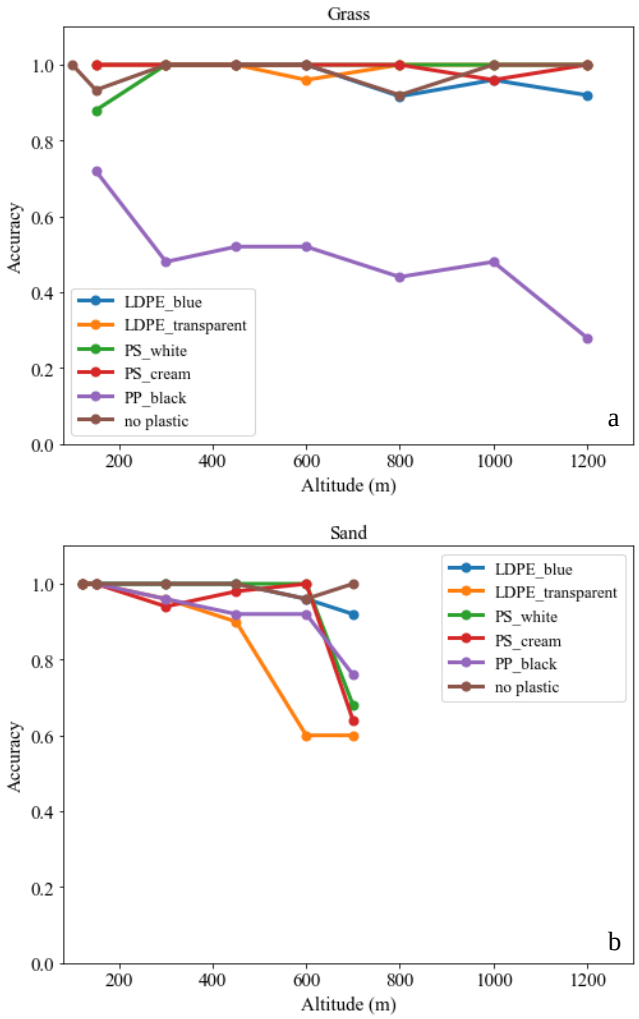

Fig. 7. Accuracy of labelling process for different materials and grass (a) and sand soil (b) as function of altitude

Due to the results shown in Fig. 7, PP black on grass soil and LDPE transparent and PP black on sand soil are further analyzed. Fig. 8 and Fig. 9 show the accuracy of the combinations with separated calculations for different percentages of coverage. It can be observed from Fig. 8 that for 100 % coverage PP black was labelled with an accuracy of 1 for altitudes $\leq$ 800 m. For 50 % coverage the accuracy was 0.8 for altitudes $\leq$ 1000 m. For 12.5 % and 6.25 % coverage the accuracy in almost all cases is $\leq$ 0.2, except for an altitude of 150 m a coverage of 12.5 %. Furthermore, as intended, one can observe a negative correlation between the coverage and the accuracy.

For LDPE transparent the accuracy is negatively correlated with the altitude, independent from the coverage percentage (Fig. 9 (a)). On the other hand, coverage percentage had an influence on the accuracy for PP black on sand soil (Fig. 9 (b)).

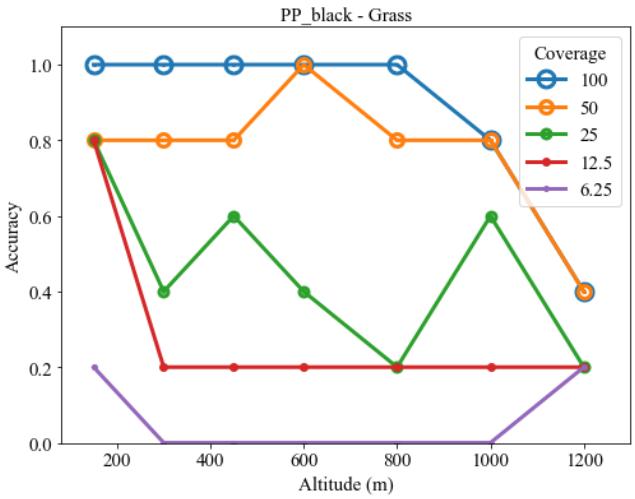

Fig. 8. Accuracy of labelling process for PP black on grass seperated for different coverages

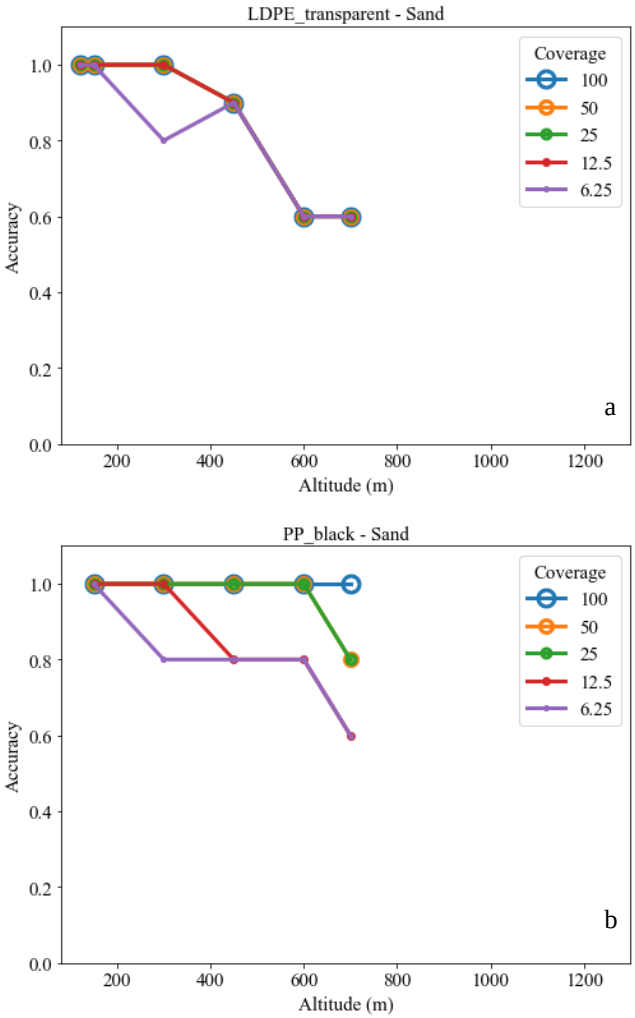

Fig. 9. Accuracy of labelling process for LDPE transparent (a) and PP black (b) on sand seperated for different coverages

The results of the labelling process are summarized in the confusion matrix given in Fig. 10. The results are split into the two different categories *No Plastic* and *Plastic*, based on the true label. It can be seen from the figure that the human achieved an accuracy of 99 % for the *No Plastic* labelled and 91 % for the *Plastic* labelled data. The overall accuracy was 92.6 %. The confusion matrix contains the total number of classifications. It needs to be noted that four labels for the *No Plastic* and two labels for the *Plastic* category are missing, because some images were not labelled by all humans.

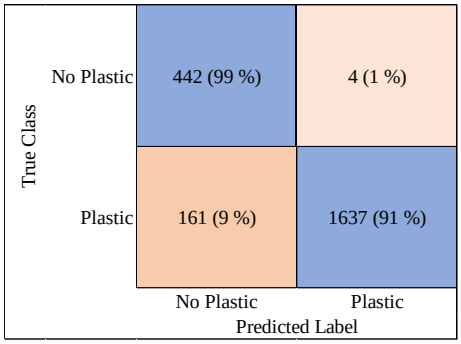

Fig. 10. Confusion matrix of human labelling process

In the second step the dataset was used to train a CNN for classifying the images. As mentioned, 20 % of the images were used as test set. These images are classified after the training of the model was completed. The total accuracy of the classifier was 93.3 %. However, the achieved accuracy differs for the two classes. The accuracy was 99 % for *Plastic* category, while it was 72 % for *No Plastic* category (Fig. 11).

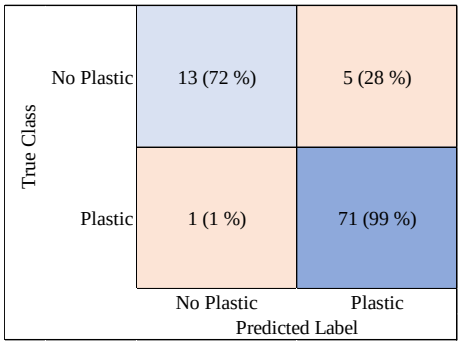

Fig. 11. Confusion matrix of CNN based binary classifier

V. Discussion

The accuracy of PP black was worse than the accuracy of the other plastic types regardless of the underlying soil (Fig. 7). Hence it can be concluded that the color of the plastic items plays an important role on the limits of detectability. In addition, decreased accuracy was shown for LDPE transparent, PS cream and PS white for sand soil compared to grass (Fig. 7 b). Thus, it can be concluded that the underlying soil has an influence on the limits of detectability.

It was shown that the accuracy depends on the coverage percentage (Fig. 8, Fig. 9 b). In contrast this dependency cannot be observed for LDPE transparent (Fig. 9 a). However, it needs to be noted that the PP black contains several smaller items, while one piece of foil was used for the LDPE transparent targets. Therefore, it can be concluded that also the item size has an influence on the detectability of plastic waste items.

Furthermore, it can be observed that both methods, i.e. human labelling and CNN classifier, show similar accuracy during the classification of the images (Fig. 10, Fig. 11). However, it needs to be noted that Fig. 10 includes five labels per image from the human labelling process, while Fig. 11 only includes one label for 20 % of the dataset, i.e. the test set. However, machine learning can be used as a tool for the classification of plastic waste from airborne remote sensing data.

VI. Conclusion and Future Work

The main ideas and initial findings of the PlasticObs+ project are presented and discussed in this work. The four different AI-systems, i.e., VIS-AI, candidate selection system, EOIR-AI and feedback loop are discussed. Different potential methods for the four subsystems are given.

In the PlasticObs+ project airborne based remote sensing is used to detect plastic waste. However, compared to recent research, images with a lower resolution will be used in this project. Therefore, a set of field tests was undertaken, using artificial plastic waste targets, to determine the limits of detectability for plastic waste. The images were classified by humans, and it was shown that both color and size of the items have an influence on the detectability. In addition, the underground plays an important role for the detectability.

A binary classifier, based on a CNN was trained to distinguish between images containing plastic and those who are not containing plastic. It was shown that this approach shows similar accuracy compared to the results from a labelling undertaken by humans. The accuracy of the binary classifier was 93.3 % while the accuracy of the labels generated by humans was 92.6 %. Hence, it can be concluded that airborne based remote sensing in combination with AI-methods can be an important tool to tackle the global plastic waste problem.

In the future, additional field test with artificial targets on different undergrounds, including water and mudflat needs to be undertaken to enhance the dataset. Furthermore, real world data of floating plastic litter will be taken using a research airplane. This data is used to train the different AI models described in section II. The trained models can be tested at the German coast using the research aircraft from Jade University of Applied Sciences. In the final step the system shall be incorporated into oil spill monitoring aircrafts and tested in different locations.

Acknowledgements

The authors would like to thank Tobias Binkele, Gizem Bulut, Michael Butter, Richard Kachel, Martin Kumm, Tobias Schmid, Jens Wellhausen, and Simone Wiegand for their support during field work and Markus Eckhardt for his support during data preparation.

REFERENCES

[1] J. R. Jambeck *et al.*, "Plastic waste inputs from land into the ocean," *Science*, vol. 347, no. 6223, pp. 768–771, Feb. 2015, doi: 10.1126/science.1260352.

[2] L. C. M. Lebreton, J. van der Zwet, J.-W. Damsteeg, B. Slat, A. Andrady, and J. Reisser, "River plastic emissions to the world's oceans," *Nat. Commun.*, vol. 8, no. 1, Art. no. 1, Jun. 2017, doi: 10.1038/ncomms15611.

[3] F. Galgani, G. Hanke, S. Werner, and L. De Vrees, "Marine litter within the European Marine Strategy Framework Directive," *ICES J. Mar. Sci.*, vol. 70, no. 6, pp. 1055–1064, Sep. 2013, doi: 10.1093/icesjms/fst122.

[4] "Directive (EU) 2019/ of the European Parliament and of the Council of 5 June 2019 on the reduction of the impact of certain plastic products on the environment".

[5] L. Recuero Virto, "A preliminary assessment of the indicators for Sustainable Development Goal (SDG) 14 'Conserve and sustainably use the oceans, seas and marine resources for sustainable development,'" *Mar. Policy*, vol. 98, pp. 47–57, Dec. 2018, doi: 10.1016/j.marpol.2018.08.036.

[6] U. N. Environment, "Global Environment Outlook 6," *UNEP - UN Environment Programme*, Apr. 03, 2019. http://www.unep.org/resources/global-environment-outlook-6 (accessed Jan. 09, 2023).

[7] K. Topouzelis, D. Papageorgiou, A. Karagaitanakis, A. Papakonstantinou, and M. Arias, "Remote Sensing of Sea Surface Artificial Floating Plastic Targets with Sentinel-2 and Unmanned Aerial Systems (Plastic Litter Project 2019)," *Remote Sens.*, vol. 12, p. 2013, Jun. 2020, doi: 10.3390/rs12122013.

[8] S. P. Garaba *et al.*, "Sensing Ocean Plastics with an Airborne Hyperspectral Shortwave Infrared Imager," *Environ. Sci. Technol.*, vol. 52, no. 20, pp. 11699–11707, Oct. 2018, doi: 10.1021/acs.est.8b02855.

[9] G. Erni-Cassola, V. Zadjelovic, M. I. Gibson, and J. A. Christie-Oleza, "Distribution of plastic polymer types in the marine environment; A meta-analysis," *J. Hazard. Mater.*, vol. 369, pp. 691–698, May 2019, doi: 10.1016/j.jhazmat.2019.02.067.

[10] R. I. Schöneich-Argent, K. Dau, and H. Freund, "Wasting the North Sea? – A field-based assessment of anthropogenic macrolitter loads and emission rates of three German tributaries," *Environ. Pollut.*, vol. 263, p. 114367, Aug. 2020, doi: 10.1016/j.envpol.2020.114367.

[11] W. He, M. Wu, M. Liang, and S.-K. Lam, "CAP: Context-Aware Pruning for Semantic Segmentation," in *2021 IEEE Winter Conference on Applications of Computer Vision (WACV)*, Waikoloa, HI, USA: IEEE, Jan. 2021, pp. 959–968. doi: 10.1109/WACV48630.2021.00100.

[12] C. Yu, C. Gao, J. Wang, G. Yu, C. Shen, and N. Sang, "BiSeNet V2: Bilateral Network with Guided Aggregation for Real-time Semantic Segmentation." arXiv, Apr. 05, 2020. Accessed: Mar. 28, 2023. [Online]. Available: http://arxiv.org/abs/2004.02147

[13] W. Chen, X. Gong, X. Liu, Q. Zhang, Y. Li, and Z. Wang, "FasterSeg: Searching for Faster Real-time Semantic Segmentation." arXiv, Jan. 16, 2020. Accessed: Mar. 23, 2023. [Online]. Available: http://arxiv.org/abs/1912.10917

[14] M. B. Pereira and J. A. dos Santos, "An End-to-end Framework For Low-Resolution Remote Sensing Semantic Segmentation." arXiv, Mar. 17, 2020. Accessed: Mar. 16, 2023. [Online]. Available: http://arxiv.org/abs/2003.07955

[15] P. R. Sokkappa, "The cost-constrained traveling salesman problem," UCRL-LR-105145, 6223080, Oct. 1990. doi: 10.2172/6223080.

[16] M. M. Flood, "The Traveling-Salesman Problem," *Oper. Res.*, vol. 4, no. 1, pp. 61–75, 1956.

[17] R. Radharamanan and L. I. Choi, "A branch and bound algorithm for the travelling salesman and the transportation routing problems," *Comput. Ind. Eng.*, vol. 11, no. 1, pp. 236–240, Jan. 1986, doi: 10.1016/0360-8352(86)90085-9.

[18] B. Golden, L. Levy, and R. Dahl, "Two generalizations of the traveling salesman problem," *Omega*, vol. 9, no. 4, pp. 439–441, Jan. 1981, doi: 10.1016/0305-0483(81)90087-6.

[19] T. Tsiligirides, "Heuristic Methods Applied to Orienteering," *J. Oper. Res. Soc.*, vol. 35, no. 9, pp. 797–809, Sep. 1984, doi: 10.1057/jors.1984.162.

[20] B. Chandra, H. Karloff, and C. Tovey, "New Results on the Old *k* -opt Algorithm for the Traveling Salesman Problem," *SIAM J. Comput.*, vol. 28, no. 6, pp. 1998–2029, Jan. 1999, doi: 10.1137/S0097539793251244.

[21] C. Tholen, L. Nolle, T. A. El-Mihoub, and O. Zielinksi, "Optimised bumblebee paths as search strategy for autonomous underwater vehicles," in *ECMS 2022 Proceedings edited by Ibrahim A. Hameed, Agus Hasan, Saleh Abdel-Afou Alaliyat*, ECMS, Jun. 2022, pp. 107–113. doi: 10.7148/2022-0107.

[22] S. Kirkpatrick, "Optimization by simulated annealing: Quantitative studies," *J. Stat. Phys.*, vol. 34, no. 5, pp. 975–986, Mar. 1984, doi: 10.1007/BF01009452.

[23] V. Chandra and A. Hareendran, *Artificial Intelligence and Machine Learning*. Delhi: PHI Learning Private Limited, 2014.

[24] C. Martin, S. Parkes, Q. Zhang, X. Zhang, M. F. McCabe, and C. M. Duarte, "Use of unmanned aerial vehicles for efficient beach litter monitoring," *Mar. Pollut. Bull.*, vol. 131, pp. 662–673, Jun. 2018, doi: 10.1016/j.marpolbul.2018.04.045.

[25] G. Gonçalves, U. Andriolo, L. Pinto, and F. Bessa, "Mapping marine litter using UAS on a beach-dune system: a multidisciplinary approach," *Sci. Total Environ.*, vol. 706, p. 135742, Mar. 2020, doi: 10.1016/j.scitotenv.2019.135742.

[26] T. Acuña-Ruz *et al.*, "Anthropogenic marine debris over beaches: Spectral characterization for remote sensing applications," *Remote Sens. Environ.*, vol. 217, pp. 309–322, Nov. 2018, doi: 10.1016/j.rse.2018.08.008.

[27] S. H. Bak, D. H. Hwang, H. M. Kim, and H. J. Yoon, "DETECTION AND MONITORING OF BEACH LITTER USING UAV IMAGE AND DEEP NEURAL NETWORK," *Int. Arch. Photogramm. Remote Sens. Spat. Inf. Sci.*, vol. XLII-3-W8, pp. 55–58, Aug. 2019, doi: 10.5194/isprs-archives-XLII-3-W8-55-2019.

[28] K. Kylili, I. Kyriakides, A. Artusi, and C. Hadjistassou, "Identifying floating plastic marine debris using a deep learning approach," *Environ. Sci. Pollut. Res.*, vol. 26, no. 17, pp. 17091–17099, Jun. 2019, doi: 10.1007/s11356-019-05148-4.

[29] M. Wolf *et al.*, "Machine learning for aquatic plastic litter detection, classification and quantification (APLASTIC-Q)," *Environ. Res. Lett.*, vol. 15, no. 11, p. 114042, Nov. 2020, doi: 10.1088/1748-9326/abbd01.

[30] A. Das and P. Rad, "Opportunities and Challenges in Explainable Artificial Intelligence (XAI): A Survey," *arXiv.org*, Jun. 16, 2020. https://arxiv.org/abs/2006.11371v2 (accessed Apr. 17, 2023).

[31] S. Budd, E. C. Robinson, and B. Kainz, "A survey on active learning and human-in-the-loop deep learning for medical image analysis," *Med. Image Anal.*, vol. 71, p. 102062, Jul. 2021, doi: 10.1016/j.media.2021.102062.

[32] Z. Li, J. Yang, Z. Liu, X. Yang, G. Jeon, and W. Wu, "Feedback Network for Image Super-Resolution," presented at the Proceedings of the IEEE/CVF Conference on Computer Vision and Pattern Recognition, 2019, pp. 3867–3876. Accessed: Apr. 17, 2023. [Online]. Available: https://openaccess.thecvf.com/content_CVPR_2019/html/Li_Feedback_Network_for_Image_Super-Resolution_CVPR_2019_paper.html

[33] J. Long, E. Shelhamer, and T. Darrell, "Fully convolutional networks for semantic segmentation," in *2015 IEEE Conference on Computer Vision and Pattern Recognition (CVPR)*, Jun. 2015, pp. 3431–3440. doi: 10.1109/CVPR.2015.7298965.

[34] K. He, X. Zhang, S. Ren, and J. Sun, "Deep Residual Learning for Image Recognition," in *2016 IEEE Conference on Computer Vision and Pattern Recognition (CVPR)*, Jun. 2016, pp. 770–778. doi: 10.1109/CVPR.2016.90.